JOC The Journal of Organic Chemistry

Article

pubs.acs.org/joc

Conformational Studies of Phe-Rich Foldamers by VCD Spectroscopy and ab Initio Calculations

Giovanna Longhi,*,† Sergio Abbate,† France Lebon,† Nicola Castellucci,‡ Piera Sabatino,*,‡ and Claudia Tomasini*,‡

†Dipartimento di Scienze Biomediche e Biotecnologie, Università degli Studi di Brescia, Viale Europa 11, 25123 Brescia, Italy, and CNISM, Consorzio Interuniversitario Scienze Fisiche della Materia, Via della Vasca Navale 84, 00146 Roma, Italy

‡Dipartimento di Chimica "G. Ciamician", Alma Mater Studiorum Università di Bologna, Via Selmi 2, I-40126 Bologna, Italy

Supporting Information

ABSTRACT: Employing VCD spectroscopy, we demonstrate that the structural behavior of the oligomers Boc-(L-Phe-L-Oxd)$_n$-OBn is similar from $n = 2$ to $n = 6$; ab initio calculations for the $n = 1$ case provide physical insight into the conformational properties. Further information is gained by IR, ^{1}H NMR, and ECD spectroscopies. ECD spectra suggest the presence of different conformations between n = 1 on one side and longer chain foldamers on the other side. VCD and absorption IR spectra in methanol solutions can be interpreted as indicative of a PPII structure. In the case of Boc-L-Phe-L-Oxd-OBn, VCD spectra in CCl_4 and detailed DFT computational analysis allow one to demonstrate that the most populated conformers exhibit backbone dihedral angles similar to those of a PPII geometry. This is a remarkable outcome, as we had previously demonstrated that the Boc-(L-Ala-D-Oxd)$_n$-OBn series folds in a β-band ribbon spiral that is a subtype of the 3_{10} helix.

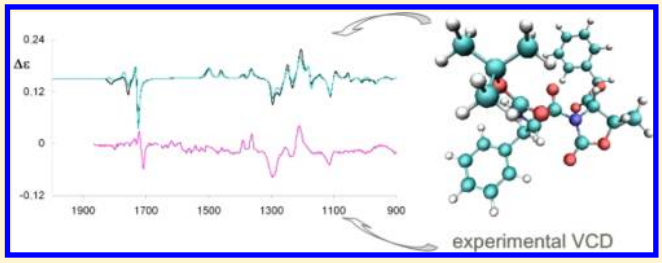

INTRODUCTION

Foldamers are oligomers that adopt specific and stable conformations similar to those typical of proteins and nucleic acids. This neologism means "folding molecules" and refers mainly to medium-sized molecules (about 500−5000 amu) that fold into definite secondary structures (i.e., helices, turns, and sheets), thus being able to mimic biomacromolecules despite their smaller size.[1] The essential requirement of a foldamer is to possess a well-defined, repetitive secondary structure, imparted by conformational restrictions of the monomeric unit.[2] Since 1996 when the neologism was coined, this research field has blossomed; many groups have explored oligomers with a wide backbone variety as potential foldamers, and several reviews have been published in this field.[3]

Our group has extensively studied the conformational behavior of oxazolidin-2-one (Oxd) containing foldamers.[4] On acylation of the Oxd units, imides are obtained: these functions behave like rigid spacers so that the two carbonyls lie apart from one another, and a *trans* conformation is imparted to the adjacent peptide bond (Figure 1).[5]

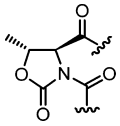

Figure 1. Preferred conformation of the imidic bond.

We have recently reported hybrid foldamers, where the Oxd moiety is alternated with an α- or a β-amino acid.[6] The relative configuration of the Oxd and the alternated amino acid is very important, since the L-Ala-D-Oxd series tends to form β-bend ribbon spirals, while the L-Ala-L-Oxd series does not. Furthermore, the insertion of the L-Phe residue alternated with the D-Oxd moiety allows us to obtain interesting compounds that behave as supramolecular materials.[7]

In this paper, we report the synthesis and the conformational analysis in solution of a series of hybrid oligomers that have the general formula Boc-(L-Phe-L-Oxd)$_n$-OBn (with n = 1, 2, 3, 4, 6). We are interested in these compounds as they are possible models for the study of amyloid fibers[8] that are constituted by peptides and are responsible for several neurodegenerative diseases, like Alzheimer's and Parkinson's disease.[9] These peptides are often rich in Phe residues, have poor solubility, and tend to lie in a very stable β-sheet structure.[10]

The conformational analysis has been carried out by ^{1}H NMR, IR, ECD (electronic circular dichroism), and VCD (vibrational circular dichroism) spectroscopy, accompanied by ab initio calculations. In particular, the latter two techniques can be very useful in the determination of the preferred secondary structure of this class of foldamers.

Received: April 16, 2012

 © XXXX American Chemical Society

RESULTS AND DISCUSSION

1. Synthesis. Boc-L-Phe-L-Oxd-OBn **1** can be prepared in high yield by addition of Boc-L-Phe-OH to L-Oxd-OBn in the presence of *N*-[(1*H*-benzotriazolyl)(dimethylamino)-methylene]-*N*-methylmethane-iminium hexafluorophosphate *N*-oxide (HBTU) and triethylamine (TEA) in dry acetonitrile, as previously reported (Scheme 1). The L-Oxd-OBn moiety (Oxd = 4-methyl-5-carboxyoxazolidin-2-one, Bn = benzyloxycarbonyl) can easily be synthesized in multigram scale starting from L-Thr.[11]

Scheme 1[a]

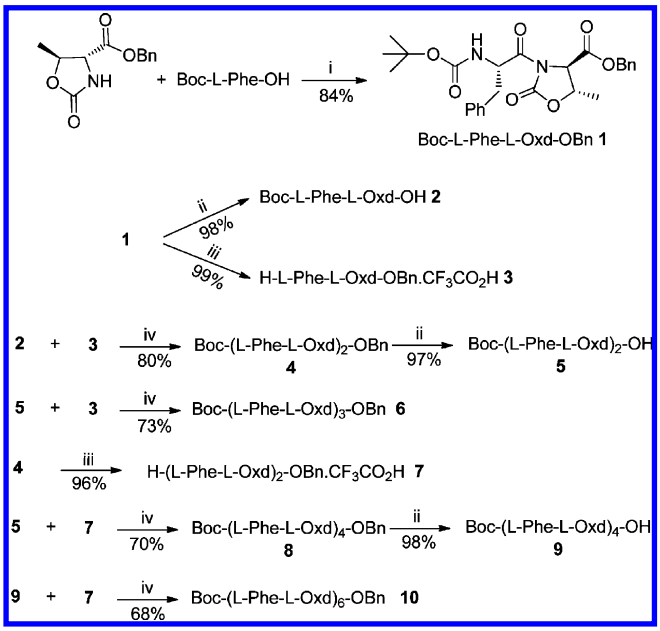

[a](i) HBTU (1.1 equiv), Et_3N (2 equiv), dry CH_3CN, t_r = 1 h; (ii) H_2, Pd/C (10%), MeOH, t_r = 16 h; (iii) TFA (18 equiv), dry CH_2Cl_2, t_r = 4 h; (iv) HBTU (1.1 equiv), Et_3N (3 equiv), dry CH_3CN, t_r = 1 h.

The oligomer series Boc-(L-Phe-L-Oxd)$_n$-OBn (n = 2, 3, 4, 6) **4**−**10** have been synthesized in solution. Boc-(L-Phe-D-Oxd)-OH **2** has been obtained by selective deprotection of the C-terminal benzyl ester with H_2 in methanol in the presence of Pd/C (5%), and H-L-Phe-D-Oxd-OBn·CF_3CO_2H **3** was prepared by cleavage of the N-terminal Boc moiety with anhydrous trifluoracetic acid (TFA) in dichloromethane (Scheme 1).

Then, **2** and **3** were coupled using HBTU and TEA in dry acetonitrile in an inert atmosphere providing **4** in satisfactory yield. By deprotection of the carbobenzoxy group with H_2 in methanol in the presence of Pd/C (5%), the corresponding acid **5** was prepared. Repetition of these two steps produces Boc-(L-Phe-L-Oxd)$_3$-OBn **6** in good yield. The longer oligomers Boc-(L-Phe-L-Oxd)$_4$-OBn **8** and Boc-(L-Phe-L-Oxd)$_6$-OBn **10** have been obtained by coupling Boc-(L-Phe-L-Oxd)$_2$-OH **5** and Boc-(L-Phe-L-Oxd)$_4$-OH **9**, respectively, with H-(L-Phe-D-Oxd)$_2$-OBn·CF_3CO_2H **7** using HBTU and TEA in dry acetonitrile.

All the deprotection steps were performed with excellent yields, while the coupling step yields were between 68 and 84%. The purification by flash chromatography of the longer oligomers proved to be difficult due to the low solubility of Boc-(L-Phe-L-Oxd)$_3$-OBn **6**, Boc-(L-Phe-L-Oxd)$_4$-OBn **8**, and Boc-(L-Phe-L-Oxd)$_6$-OBn **10** in any solvent, as all the products were blocked in the silica gel and the yields dramatically decreased. This obstacle was overcome by performing the purification with the help of an ultrasound bath. The reaction crude was dissolved in ethyl acetate and washed with water to eliminate the water-soluble byproduct (HOBt in part, unreacted amines and acids, etc.), and then it was concentrated and the solvent replaced with cyclohexane. This mixture was sonicated so that the byproduct, tetramethylurea, and the remaining part of HOBt dissolved in the apolar solvent, and the desired product could be recovered pure after filtration. Following this procedure, the oligomers **6**, **8**, and **10** were obtained pure in satisfactory yields.

2. Conformational Analysis. Information on the preferred conformation of the oligomers in solution was obtained by the analysis of FT-IR, ^{1}H NMR, ECD, and VCD absorption spectra and by DFT (density functional theory) quantum chemical calculations on Boc-L-Phe-L-Oxd-OBn.

In particular, FT-IR and ^{1}H NMR spectroscopy helped us to understand if any intramolecular N−H···O═C hydrogen bonds are formed, while CD spectroscopy provided us with some interesting information on the preferred secondary structure. Finally, DFT calculations on **1** are presented with a detailed conformational analysis validated by comparison with VCD data in an apolar solvent like CCl_4.

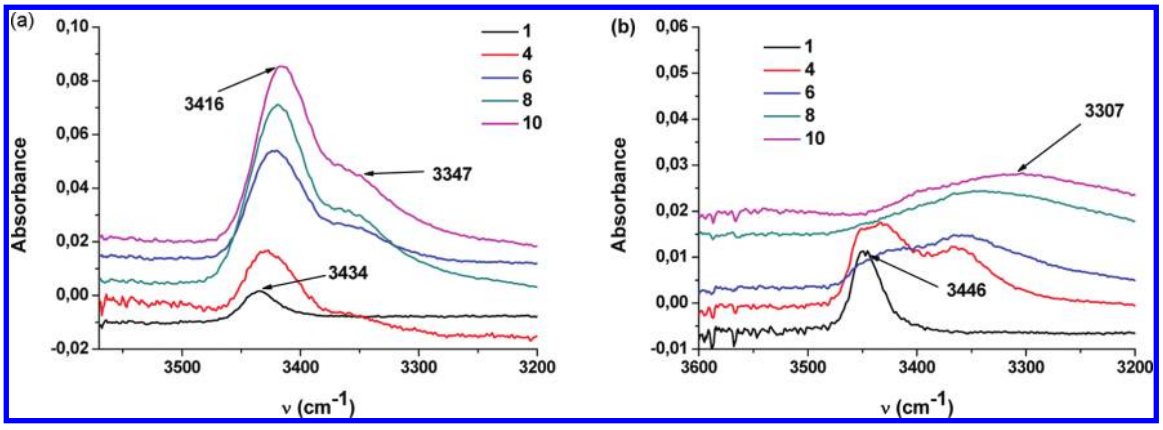

Figure 2. (a) N−H stretching regions of the IR absorption spectra for 3 mM samples of oligomers **1**, **4**, **6**, **8**, and **10** in CH_2Cl_2 at room temperature. (b) N−H stretching regions of the IR absorption spectra for 3 mM samples of oligomers **1**, **4**, **6**, **8**, and **10** in CCl_4 at room temperature.

2.1. IR Spectroscopy. The analysis of the N−H stretching regions helps one to detect if intramolecular N−H···O═C hydrogen bonds are formed, since nonhydrogen-bonded amide NH bonds exhibit a stretching signal above 3400 cm^{-1}, while hydrogen-bonded amide NH bonds[12] produce a stretching band below 3400 cm^{-1}.

The FT-IR spectra were recorded for 3 mM solutions in both methylene chloride (aprotic polar solvent) and carbon tetrachloride (apolar solvent). This low concentration was chosen in order to avoid possible self-aggregation and due to the low solubility of the longer oligomers **6**, **8**, and **10**. Figure 2 shows the FT-IR absorption spectra of the oligomers **1**, **4**, **6**, **8**, and **10** in methylene chloride and carbon tetrachloride.

For all compounds in methylene chloride, a strong band above 3400 cm^{-1} is noticed indicating that no hydrogen bond is formed (Figure 2a). A shoulder centered below 3400 cm^{-1} (about 3340 cm^{-1}) appears for **4**, **6**, **8**, and **10**: it becomes stronger with increasing foldamer chain length but never becomes the main stretching band. The formation of this shoulder suggests that equilibrium takes place among different conformations. In an apolar solvent, like carbon tetrachloride, the results are quite different: while for compound **1**, only one band centered at 3446 cm^{-1} is observed, for longer oligomers, a broad band centered at about 3300 cm^{-1} appears (Figure 2b). This effect may be due to equilibrium between structures, or it simply could be ascribed to the formation of intermolecular hydrogen bonds due to the self-aggregation of these compounds in apolar solvents.

2.2. ^1H NMR Spectroscopy. The occurrence of intramolecular C═O···H−N hydrogen bonds was checked also by investigating the dependence of the NH proton chemical shifts on an increasing percentage (up to 10%) of DMSO-d_6 in a 3 mM $CDCl_3$ solution. DMSO is a strong hydrogen-bond acceptor, and if DMSO is bound to a free NH proton, a considerable downfield shift of the proton signal can be expected.[13]

The $\Delta\delta$ values (difference of NH proton chemical shifts for the spectra recorded in pure $CDCl_3$ and in 9:1 $CDCl_3$/DMSO-d_6) for NH hydrogens of oligomers Boc-(L-Phe-L-Oxd)$_n$-OBn **6**, **8**, and **10** are summarized in Table 1 (see Figure S1 of the Supporting Information). All the hydrogen amides have $\Delta\delta$ values above 1.8 ppm: these values are very high and account for non-hydrogen-bonded NH amide protons. In any case, it is worth mentioning that the NH-Boc hydrogens have small $\Delta\delta$ values that become smaller as the foldamer becomes longer.[14]

Table 1. $\Delta\delta$ (ppm)[a] for NH Titration for Oligomers Boc-(L-Phe-L-Oxd)$_n$-OBn with n = 3, 4, and 6

compound	NH-Boc	NH_1	NH_2	NH_3	NH_4	NH_5
6	0.19	1.98	2.08			
8	0.10	1.98	2.05	2.07		
10	0.08	1.85	1.99	1.96	1.97	2.16

[a]Difference of NH proton chemical shifts between the spectrum recorded in pure $CDCl_3$ and in 9:1 $CDCl_3$/DMSO-d_6.

Unfortunately, these compounds are either waxy or amorphous solids, so no crystal suitable for X-ray diffraction analysis could be grown to allow a direct determination of the preferred conformation of this class of oligomers (see Figure S2 of the Supporting Information). For this reason, we resorted to ECD (electronic circular dichroism) and VCD (vibrational circular dichroism) measurements, which together with DFT calculations may provide interesting information on the preferred conformations of the oligomers.

2.3. ECD Spectroscopy. Electronic circular dichroism spectroscopy was used in a preliminary conformational analysis of the homochiral oligomers Boc-(L-Phe-L-Oxd)$_n$-OBn (n = 1, 2, 3, 4, 6), compounds **1**, **4**, **6**, **8**, and **10**, respectively, based on their electronic transitions. ECD measurements were recorded for 1 mM methanol solutions at room temperature for all compounds. The overlap of the spectra of **1**, **4**, **6**, **8**, and **10**, normalized per residue, is reported in Figure 3 and exhibits, for all foldamers, a positive band centered at 195 nm, due to either the peptide transition or the strong B transitions of Phe that are usually located around 188 nm.

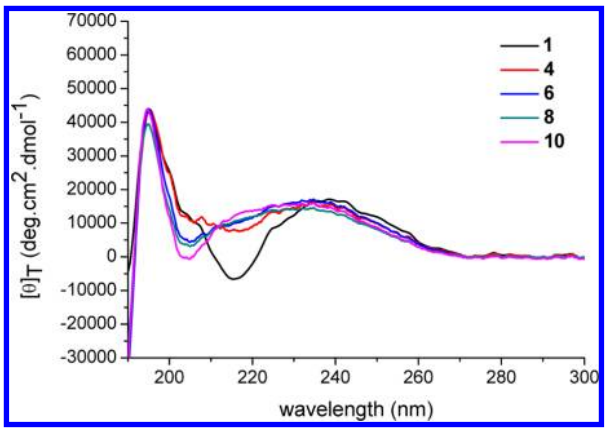

Figure 3. Normalized per-residue ECD spectra of the Boc-(L-Phe-L-Oxd)$_n$-OBn (n = 1−6) series in MeOH solution (1 mM).

The ECD spectra of compound **1** display a negative signal at ca. 215 nm and a strong positive band at 195 nm, while at 190 nm, a negative ellipticity value is shown (see Figure S3 of the Supporting Information). In addition, a broad positive unfeatured band between 270 and 220 nm (crossover points) is displayed and may be attributed to the aromatic contribution of the Phe residue, a strongly absorbing chromophore. Phe chromophore contributions, L_a, are reported to fall in the peptide region at 208 nm,[15] or at 225−230 nm.[16] The L_b phenylalanine transition, on the other hand, occurs at 257 nm.

Some spectral features of longer oligomers are probably due to a mixture of conformers present in solution. It is clear from Figure 3 that the negative feature at 215 nm in **1** becomes weaker and blue shifted with increasing chain length (in **10** it falls at 205 nm). A similar blue shift is shown by the positive broad band from 238.5 nm in **1** to 234.0 nm in **10** (see Figures S3 and S4 of the Supporting Information). These spectral features seem to rule out the possibility of a self-assembly of the oligomer, driven by the stacking interaction of aromatic units,[17] while a PPII conformation could be taken into account supported by the fact that the broad band due to the aromatic chromophore contributions (with its maximum at 234 nm) could hide the characteristic positive peak around 220 nm.

2.4. VCD Spectroscopy. In order to gain further information regarding the preferred conformations of these systems, we also recorded VCD spectra in the mid-IR region. VCD has been around since 1975,[18,19] for almost the same amount of time as ECD, but has become a handy tool for absolute-configuration determination as well as for conformational analysis, after extension of the accessible frequency range to mid-IR and after the use of ab initio calculations has allowed impeccable and

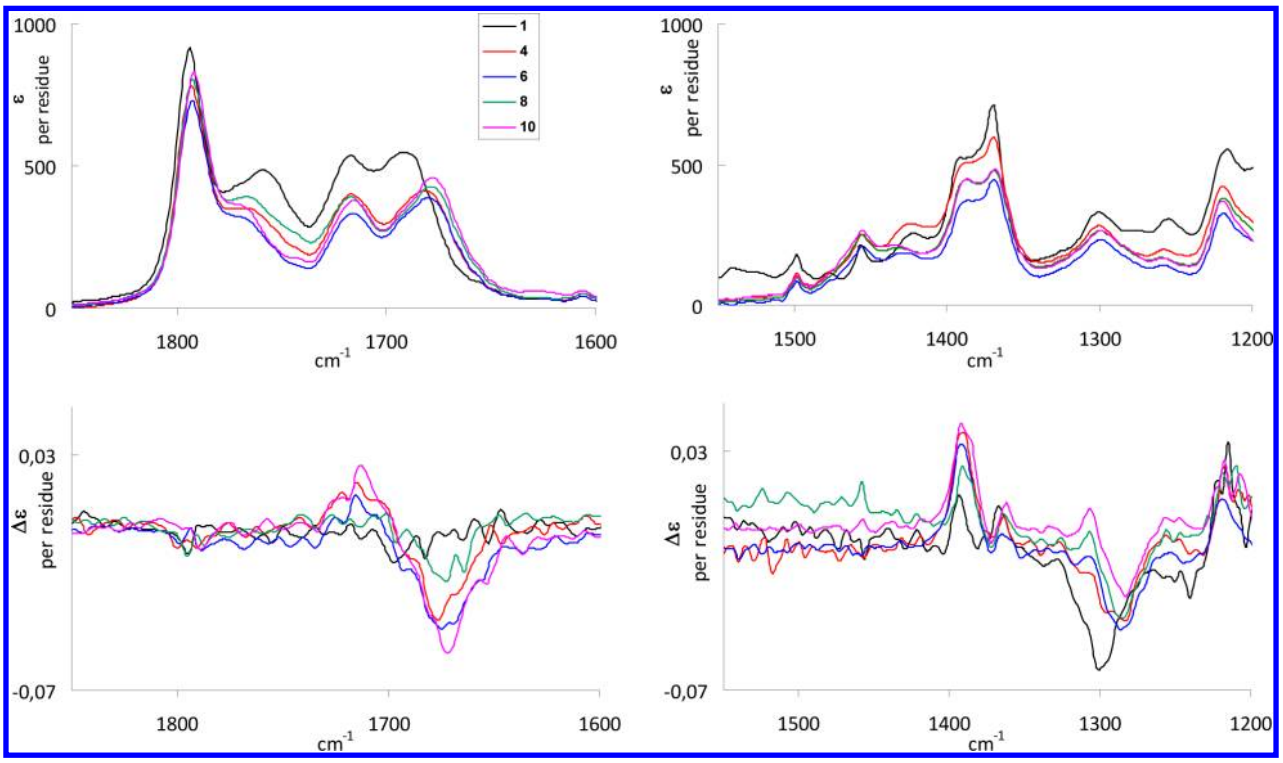

Figure 4. IR and VCD spectra of the Boc-(L-Phe-L-Oxd)$_n$-OBn (n = 1, 2, 3, 4, 6) series in methanol-d_4. The ε and $\Delta\varepsilon$ are presented in residue units (see text).

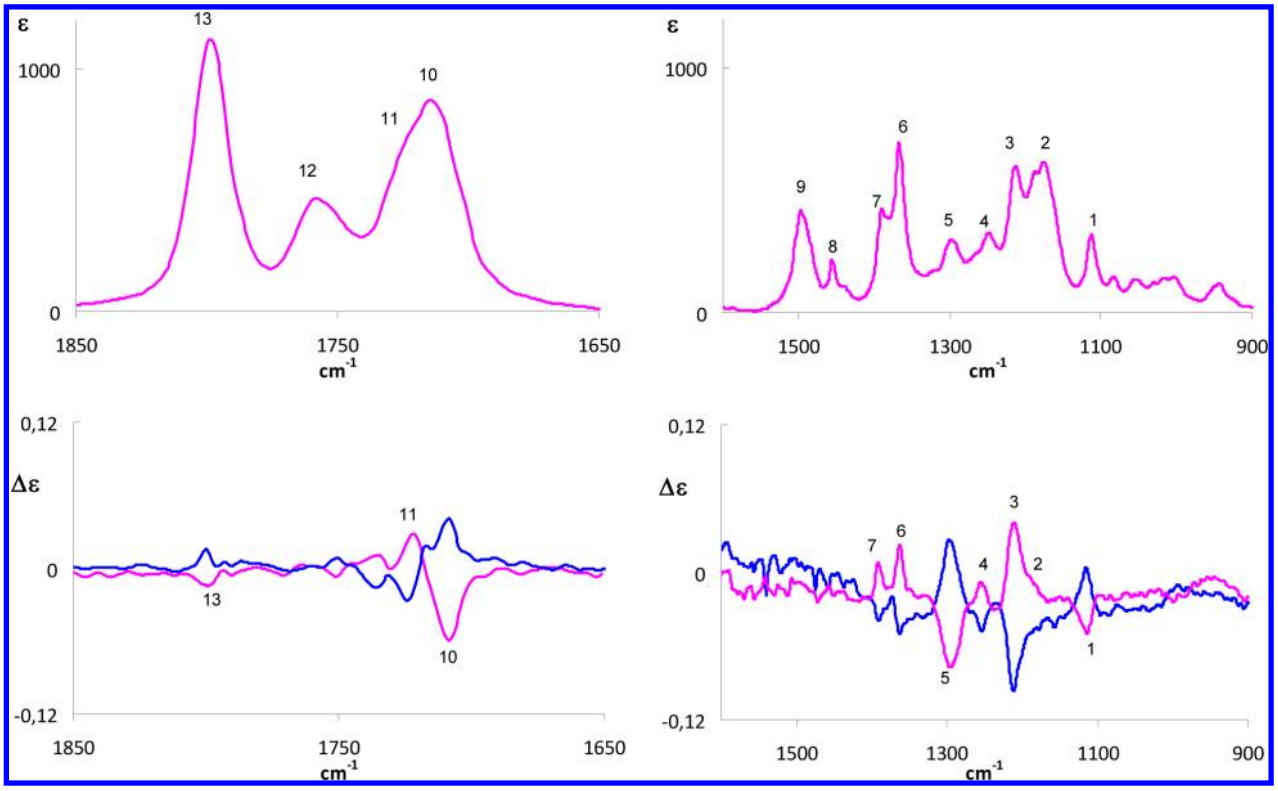

Figure 5. IR (top) and VCD (botton) spectra of Boc-L-Phe-L-Oxd-OBn **1** (pink trace) and of the enantiomer Boc-D-Phe-D-Oxd-OBn (blue trace) in CCl_4 (20 mM solution). Numbers are introduced to facilitate correspondence between IR and VCD.

easy interpretation of VCD spectra in the mid-IR range, in frequency, sign, and intensity.[20−25] Besides, as mentioned above, this technique is particularly adequate for the systems under study since they contain aromatic amino acids. As explained above, aromatic ECD chromophores interfere with the signals characteristic of the amino groups, which are usually associated with backbone conformations of peptides and proteins.

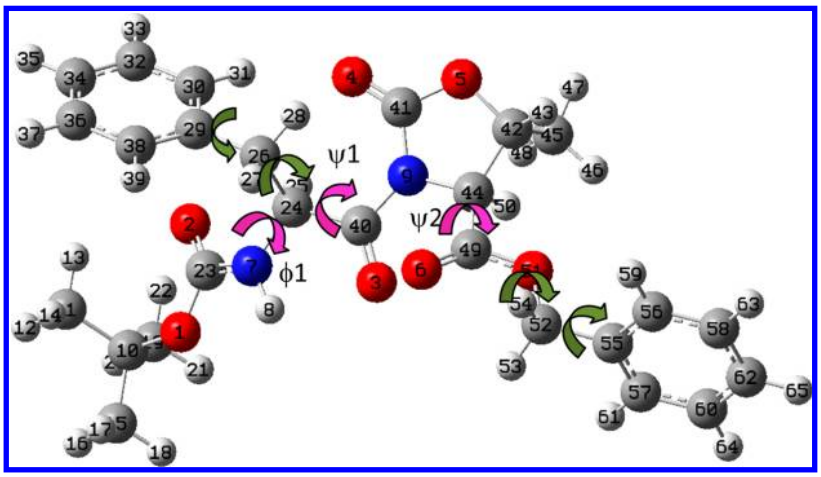

Figure 6. Atom numbers and definition of dihedral angles (in degrees) for compound **1**. ϕ_1: 23, 7, 24, 40. ψ_1: 7, 24, 40, 9. τ_{Pro}(*trans*−*cis* Pro): 44, 9, 40, 24. ψ_2: 9, 44, 49, 51. χ_{1Phe1}: 7, 24, 26. χ_{2Phe1}: 24, 26, 29, 30. τ_{COOBn}: 44, 49, 51, 52. χ_{1Bn}: 49, 51, 52, 55. χ_{2Bn}: 51, 52, 55, 56. ϕ_2 is not reported since it has a fixed value as explained in the text.

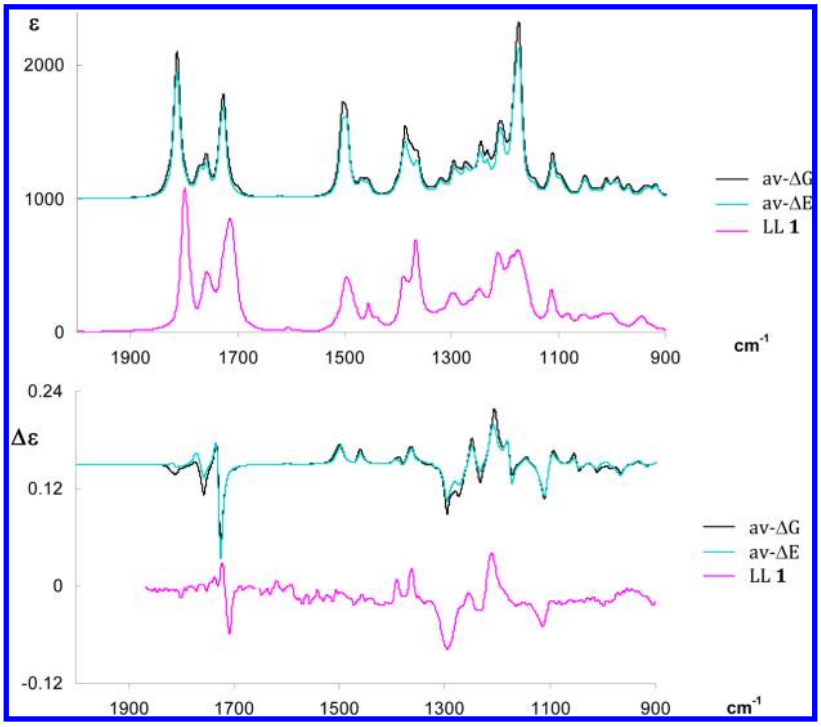

Figure 7. Comparison of experimental IR (top) and VCD (bottom) spectra of **1** with the corresponding Boltzmann average calculated spectra.

VCD measurements were recorded at room temperature for 20 mM solutions in carbon tetrachloride for **1**; for longer oligomers the solubility in this solvent is too low to obtain VCD spectra. For this reason all Boc-(L-Phe-L-Oxd)$_n$-OBn compounds (n = 1, 2, 3, 4, 6) were considered in 20 mM CD_3OD solutions. The concentrations needed in VCD spectroscopy are actually quite large, and this should be kept in mind when comparing with the previous analysis based on the ECD and IR of dilute solutions.

A qualitative comparison of the VCD spectra recorded in methanol, with help from the literature data on peptides, can be carried out. In Figure 4 we report the IR and VCD spectra for all oligomers in the L form. To provide evidence for the differences in the behavior of different-sized foldamers, we normalized IR and VCD spectra, dividing ε and $\Delta\varepsilon$ by n, for each Boc-(L-Phe-L-Oxd)$_n$-OBn considered. The more traditional comparison in the original ε and $\Delta\varepsilon$ scales is given in Figure S5 of the Supporting Information. We distinguish the two regions: 900−1600 cm^{-1} on the right side and 1600−1800 cm^{-1} on the left side (the latter contains the carbonyl stretching modes coupled with the NH in-plane bending modes, defining the amide I modes, which are so often used in the study of peptides and proteins[26]). The most prominent VCD bands are observed at 1215 cm^{-1} having a positive sign (+), 1280 (−) (1300 cm^{-1} for **1**), 1390 (+), 1675 (−), and 1710 cm^{-1} (+). Regarding the amide I bands, the negative feature at 1675 cm^{-1}, dominating over the positive component at higher frequency, may be suggestive of β structures for compounds **4**, **6**, **8**, and **10**. However, in usual amino-acidic peptides, this band appears at wavenumbers lower than 1650 cm^{-1};[22,27,28] the copresence of a positive component at higher energy is compatible with PPII-type conformations, which in the case of peptides present

precisely a couplet. The fact that observed wavenumbers do not correspond to the values usually observed for peptides can be attributed to the Oxd unit.

Both IR and VCD spectra of compound **1** are somewhat different from those of the longer foldamers, in agreement with ECD findings.

To gain further information on these systems and to verify the latter observation, we recorded VCD spectra also in CCl_4 for compound **1**, which can be dissolved in sufficient amount.

The VCD spectra of the two enantiomers are reported in the bottom part of Figure 5, while in the top part we provide the corresponding IR spectra; still we distinguish the two regions 1600−900 and 1600−1800 cm^{-1}.

The shape of the IR spectrum presents differences with respect to the one in methanol; in particular the band at 1690 cm^{-1} is not present. This suggests that, as expected, the preferential conformations are strongly dependent on the solvent nature.

2.5. DFT Calculations. In order to understand the preferred conformation adopted by monomer **1** in an apolar solvent, DFT calculations have been performed to simulate its VCD spectrum. The data from CCl_4 can be considered representative of the isolated molecule, i.e., interactions with solvent molecules are expected to be small. For this reason, such data are the easiest ones to simulate and calculations in vacuo can be considered a good approximation.[21] We performed DFT calculations on compound **1** by first optimizing geometries and then by calculating vibrational frequencies, normal modes, and infrared and VCD intensities (dipole and rotational strengths), allowing us to finally simulate spectra for due comparison with experimental data (based on the assumption of Lorentzian bandshapes with a 12 cm^{-1} width). The relevant conformational degrees of freedom for compound **1** are shown in Figure 6 where the backbone dihedral angles ϕ_1, ψ_1, and ψ_2 have been systematically varied. The dihedral angle, ϕ_2, assumes values of ∼70°, and the Oxd group is approximately in the *trans* position (we checked that the *cis* conformation, which is possible for proline, is quite improbable due to repulsion between two carbonyl groups). Also, the two torsional angles, χ_1 and χ_2, for each of the two phenyl groups have been varied. The conformational search has been conducted at the PM3 level and at the B3LYP/6-31+G** level. Vibrational mode analysis ensures that the optimized geometries are local minima and permit evaluation also of Gibbs free energies for the various conformers. In Table S1 of the Supporting Information, we report the list of the 15 lowest-energy conformers with relative populations obtained, by considering energy (second column), Gibbs free energy values (third column), and the values for all relevant dihedral angles.

The complete set of calculated IR and VCD spectra corresponding to the geometrical structures of Table 1 are reported in Figure S6 of the Supporting Information, while in Figure 7 we show only the comparison of the Boltzmann weighted averages of the calculated spectra with the experimental data. The calculated spectra (absorption and VCD) of Figure S6 of the Supporting Information are reported in order of decreasing population factors based on ΔG from bottom to top, compared to the experimental one in CCl_4 (bottom trace). In the figure, when calculated spectra refer to conformations with similar ϕ_1 and ψ_1 angles, the same color has been used. In fact, one can observe that similar ϕ_1 and ψ_1 backbone angles are related to similar, yet nonidentical, spectra. We have identified three instances: red for PPII-like angle values ($\phi_1 \approx -70°$, $\psi_1 \approx 150°$), green for β-structure-like angles ($\phi_1 \approx -150°$, $\psi_1 \approx 150°$), and blue for angle values appropriate to a helix ($\phi_1 \approx -100°$, $\psi_1 \approx -50°$). The most populated conformers exhibit VCD and IR spectra resembling the experimental ones; this is important since it means that the calculated geometries and populations adequately represent the situation in CCl_4 solution.

From Table S1 and Figure S6 of the Supporting Information, we may conclude that the two most-populated conformers A and B (red spectra) exhibit values for the ϕ_1 and ψ_1 angles typical of a PPII helix[29] (the PPII and β structures have similar ψ but different ϕ values). All conformers with similar PPII-type ϕ_1 and ψ_1 values give the negative, observed intense band at about 1710 cm^{-1}. Other structures whose population is non-negligible (C and D in the table with green spectra in Figure S6 of the Supporting Information) show calculated spectra which do not exhibit the negative band at ca. 1710 cm^{-1} (clearly observed as #10 in Figure 5) but present all correct features observed in the range 1200−1300 cm^{-1}. The former band at 1710 cm^{-1} can be attributed to the amide I mode, which is normally taken as a marker of peptide secondary structure;[30] it has the aspect of a strong negative band at lower frequencies followed by a positive feature at higher frequencies. In agreement with literature data,[28,31] we may recognize the signature of a PPII structure. We notice, however, that the frequency is much higher than the standard amide I frequency (ca. 1650 cm^{-1}); this may be due to both the short foldamer length and the presence of the non-amino-acidic group, Oxd. For all populated conformers the assignment of the bands observed between 1700 and 1800 cm^{-1} is the following (for the band numbering see Figure 5): 10 and 11, amide I vibrations of the two peptidic carbonyls; 12, carbonyl stretching adjacent to the terminal OBn; and 13, the carbonyl stretching of the Oxd ring. We remark that this spectroscopic region is not perturbed by phenyl signals. The calculated frequencies of aromatic ring vibrations are lower than 1700 cm^{-1}, and their calculated rotational strengths are very small in this region.

The good correspondence between calculated and experimental IR and VCD spectra can be checked in Figure 7, where the averages of spectra weighted with ΔG and ΔE Boltzmann factors are reported. In conclusion, considering the overall spectrum, we maintain that the observed VCD signals are compatible with the lower-energy conformers whose backbone angles are consistent with a PPII or a β geometry, but different from higher-energy conformers with ϕ_1 and ψ_1 angles appropriate for α or 3_{10} helices. We reiterate, though, that the description given is just indicative of the backbone dihedral angles assumed by Boc-L-Phe-L-Oxd-OBn **1**, which is too short to show a real peptide secondary structure.

On the same conformers examined by VCD, we also calculated ECD spectra via the TD-DFT methodology, using the functional CAM-B3LYP and 6-31+G** basis set. We present these calculations in Figure S7 of the Supporting Information and report in Figure 8 the averages of the calculated spectra weighted with ΔG and ΔE Boltzmann factors. It is reassuring to notice how the most populated conformers show the positive band attributable to the Phe transitions as experimentally observed. In any case we are conscious that the comparison of in vacuo calculations with experiments carried out in methanol is not fully appropriate: solvent effect is quite important as was also concluded from the fact that the amide I VCD signals recorded in CCl_4 (Figure 5) are not observed in methanol (Figure 4).

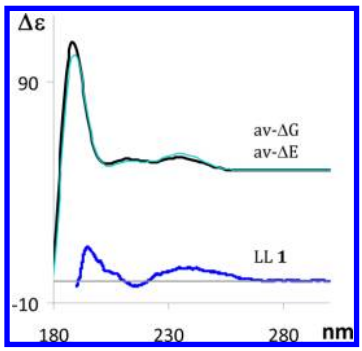

Figure 8. Comparison of experimental ECD (bottom) spectra of **1** with the corresponding Boltzmann average calculated spectra.

■ CONCLUSIONS

The oligomers of the Boc-(L-Phe-L-Oxd)$_n$-OBn series have been synthesized in solution in high yield and have been purified by means of ultrasound irradiation. This technique allowed us to avoid the purification through flash chromatography that strongly reduces the yields. Then, employing several experimental techniques we demonstrated that the structural behavior of the oligomers Boc-(L-Phe-L-Oxd)$_n$-OBn are similar from n = 2 to n = 6. An analysis of ECD spectra of the oligomers recorded in methanol, although not leading to a clear-cut conclusion with respect to foldamer conformation being perturbed by aromatic contributions, suggests the presence of different conformations for **1**, on one side, and longer chain foldamers, on the other side, as clearly shown by the significant blue shift of both the negative and the positive ECD bands with increasing chain length.

VCD and absorption IR spectra in methanol solutions suggest the formation of PPII structure, particularly due to the presence of a positive signal above 1700 cm^{-1} and a negative one at lower wavenumbers. This indication is given in analogy to what was observed for peptides: the fact that the band wavenumbers observed here do not correspond to literature data for real peptides is due to the presence of the Oxd groups.

In any case, since we are not dealing with peptides, assignment and interpretation of the spectra must rely also on calculations. Detailed DFT computational analysis has been conducted for Boc-L-Phe-L-Oxd-OBn. This short model presents a low number of possible conformers and can be treated theoretically as a molecule in vacuo since it can be dissolved in CCl_4 in which the VCD experiments are run. The most populated conformers have been identified; they exhibit backbone dihedral angles in the same range as those of a PPII geometry. Oxd−carbonyl presents the highest stretching frequency, but also vibrations involving backbone C═O stretchings show quite a high wavenumber value. The amide I region of the absorption and VCD spectra is not perturbed by aromatic contributions.

The above conformational assignment is a remarkable outcome as we had demonstrated in the past that the Boc-(L-Ala-D-Oxd)$_n$-OBn series folds in a β-band ribbon spiral, that is a subtype of the 3_{10} helix. This finding has been predicated mainly on the basis of VCD, which has been applied here for the first time to study these foldamer systems.

■ EXPERIMENTAL SECTION

Synthesis. The melting points of the compounds were determined in open capillaries and are uncorrected. High-quality infrared spectra (64 scans) were obtained at 2 cm^{-1} resolution using a 1 mm NaCl solution cell and a FT-IR spectrometer. All spectra were obtained in 3 mM solutions in dry CH_2Cl_2 at 297 K. All compounds were dried in vacuo, and all the sample preparations were performed in a nitrogen atmosphere. Routine NMR spectra were recorded with spectrometers at 400 MHz (^{1}H NMR) and 100 MHz (^{13}C NMR). The measurements were carried out in CD_3OD and in $CDCl_3$. The proton signals were assigned by gCOSY spectra. Chemical shifts are reported in δ values relative to the solvent (CD_3OD or $CDCl_3$) peak.

Boc-L-Phe-L-Oxd-OBn 1. A solution of Boc-L-Phe-OH (0.50 g, 1.89 mmol) and HBTU (0.72 g, 1.89 mmol) in dry acetonitrile (40 mL) was stirred in a nitrogen atmosphere for 10 min at room temperature. Then L-Oxd-OBn (0.44 g, 1.89 mmol) in dry acetonitrile (10 mL) was added dropwise at room temperature, followed by Et_3N (3.78 mmol, 0.52 mL). The solution was stirred for 50 min in a nitrogen atmosphere, and then acetonitrile was removed under reduced pressure and replaced with ethyl acetate. The mixture was washed with brine (1 × 30 mL), 1 N aqueous HCl (1 × 30 mL), and a concentrated solution of $NaHCO_3$ (1 × 30 mL), dried over sodium sulfate, and concentrated in vacuo. The product was obtained pure after silica gel chromatography (90:10 *c*-Hex/ethyl acetate → 70:30 *c*-Hex/ethyl acetate as eluant) in 84% (0.77 g) overall yield as a waxy solid. $[\alpha]_D$: −2.1 (*c* 1.0, $CHCl_3$). IR (CH_2Cl_2, 3 mM): ν = 3442, 1799, 1761, 1738, 1717 cm^{-1}. IR (solid, 1% in KBr): ν 3354, 3436, 3354, 1791, 1739, 1725, 1690 cm^{-1}. ^{1}H NMR ($CDCl_3$): δ 1.25 (s, 9H, *t*-Bu), 1.48 (d, 3H, Me, *J* = 6.4 Hz), 2.50 (dd, 1H, *J* = 9.6, 13.6 Hz, C*H*H-Ph), 3.22 (dd, 1H, *J* = 3.3, 13.6 Hz, CH*H*-Ph), 4.50−4.58 (m, 2H, CHN-Oxd + CHO-Oxd), 4.84 (d, 1H, *J* = 8.8 Hz, NH), 5.16 (AB, 2H, *J* = 12.4 Hz), 5.57 (dt, 1H, *J* = 4.0, 9.6 Hz), 7.12−7.33 (m, 10H, 2 × Ph). ^{13}C NMR ($CDCl_3$): δ 28.0, 37.6, 53.9, 67.7, 67.8, 73.3, 73.6, 79.6, 126.6, 126.8, 128.1, 128.2, 128.3, 128.6, 129.3, 134.3, 135.8, 151.3, 155.0, 167.5. Anal. Calcd for $C_{26}H_{30}N_2O_7$: C, 64.72; H, 6.27; N, 5.81. Found: C, 64.69; H, 6.25; N, 5.78.

Boc-L-Phe-L-Oxd-OH 2. Compound **1** (0.72 mmol, 0.48 g) was dissolved in MeOH (30 mL) under nitrogen. C/Pd (35 mg, 10% w/w) was added under nitrogen. A vacuum was created inside the flask using the vacuum line. The flask was then filled with hydrogen using a balloon (1 atm). The solution was stirred for 16 h under a hydrogen atmosphere. The product was obtained pure in 98% yield (0.28 g) as an oil, after filtration through filter paper and concentration in vacuo. ^{1}H NMR (CD_3OD): δ 1.37 (s, 9H, *t*-Bu), 1.62 (d, 3H, Me, *J* = 6.4 Hz), 2.71 (dd, 1H, *J* = 10.8, 14.0 Hz, C*H*H-Ph), 3.35 (m, 1H, CH*H*-Ph), 4.65 (d, 1H, *J* = 4.4 Hz, CHN-Oxd), 4.80 (m, 1H, CHO-Oxd), 5.59 (dd, 1H, *J* = 3.2, 10.8 Hz), 7.21−7.44 (m, 5H, Ph). ^{13}C NMR (CD_3OD): δ 21.2, 28.6, 38.2, 56.2, 62.9, 76.0, 80.7, 127.7, 129.3, 130.4, 138.5, 153.8, 158.0, 171.3, 174.3. Anal. Calcd for $C_{19}H_{24}N_2O_7$: C, 58.16; H, 6.16; N, 7.14. Found: C, 58.13; H, 6.19; N, 7.12.

H-L-Phe-L-Oxd-OBn·CF_3CO_2H 3. A solution of **1** (0.52 mmol, 0.25 g) and TFA (9.36 mmol, 0.720 mL) in dry methylene chloride (20 mL) was stirred at room temperature for 4 h; then the volatiles were removed under reduced pressure, and the corresponding amine salt was obtained pure in 99% yield (0.26 g) as a waxy solid, without further purification. ^{1}H NMR ($CDCl_3$): δ 1.52 (d, 3H, Me, *J* = 3.96 Hz), 2.77 (dd, 1H, *J* = 9.2, 14.4 Hz, C*H*H-Ph), 3.37 (dd, 1H, *J* = 3.8, 14.4 Hz, CH*H*-Ph), 4.51−4.64 (m, 2H, CHN-Oxd + CHO-Oxd), 5.15 (AB, 2H, *J* = 11.6 Hz), 5.57 (m, 1H, NH), 7.08−7.40 (m, 10H, 2 × Ph). ^{13}C NMR ($CDCl_3$): δ 19.6, 19.8, 35.2, 53.8, 60.1, 60.3, 65.0, 67.6, 67.7, 73.5, 73.9, 127.4, 127.5, 127.6, 127.8, 128.0, 128.3, 128.4, 128.5, 131.5, 133.2, 150.4, 159.6 (q, CF_3), 166.0, 167.8. Anal. Calcd for $C_{23}H_{23}F_3N_2O_7$: C, 55.65; H, 4.67; N, 5.64. Found: C, 55.68; H, 4.68; N, 5.61.

Boc-(L-Phe-L-Oxd)$_2$-OBn 4. A solution of **2** (0.20 g, 0.52 mmol) and HBTU (0.20 g, 0.52 mmol) in dry acetonitrile (20 mL) was stirred in a nitrogen atmosphere for 10 min at room temperature. Then a mixture of **3** (0.52 mmol) and Et_3N (1.56 mmol, 0.22 mL) in dry acetonitrile (10 mL) was added dropwise at room temperature. The solution was stirred for 50 min in a nitrogen atmosphere, and then acetonitrile was removed under reduced pressure and replaced with ethyl acetate. The mixture was washed with brine (1 × 30 mL), 1 N aqueous HCl (1 × 30 mL), and a concentrated solution of $NaHCO_3$ (1 × 30 mL), dried over sodium sulfate, and concentrated in vacuo.

The product was obtained pure after silica gel chromatography (90:10 *c*-Hex/ethyl acetate → 70:30 *c*-Hex/ethyl acetate as eluant) in 80% yield (0.32 g) as a white solid. Mp: 81−82 °C. $[\alpha]_D^{20}$: −26 (*c* 1.0, $CHCl_3$). IR (CH_2Cl_2, 3 mM): ν 3427, 1789, 1752, 1711 cm^{-1}. IR (solid, 1% in KBr): ν 3362, 1785, 1752, 1707 cm^{-1}. ^1H NMR ($CDCl_3$): δ 1.22−1.30 (m, 15H, 2 × Me + *t*-Bu), 2.46−2.59 (m, 2H, 2 × CHH-Ph), 3.08−3.46 (m, 2H, 2 × CHH-Ph), 4.12−4.68 (m, 4H, 2 × CHN-Oxd + 2 × CHO-Oxd), 4.89 (bs, 1H, NH), 5.06−5.24 (m, 2H, OCH_2Ph), 5.44−5.60 (m, 1H, CHN-CH_2Ph), 5.86−5.93 (m, 1H, CHN-CH2Ph), 6.63 (d, 1H, *J* = 8.4 Hz, NH), 6.89−7.47 (m, 15H, 3 × Ph). ^{13}C NMR ($CDCl_3$): δ 14.2, 20.4, 21.0, 21.2, 26.9, 27.8, 28.2, 37.9, 53.0, 54.2, 55.4, 60.4, 61.2, 61.5, 62.6, 68.3, 73.9, 74.2, 79.8, 80.2, 126.7, 126.8, 127.0, 127.1, 127.2, 128.4, 128.5, 128.8, 129.5, 130.1, 134.4, 135.7, 136.1, 151.4, 151.6, 155.2, 158.7, 163.8, 166.7, 166.9, 167.5, 167.7, 171.2, 171.3, 171.7, 171.9, 172.7, 173.4. Anal. Calcd for $C_{40}H_{44}N_4O_{11}$: C, 63.48; H, 5.86; N, 7.40. Found: C, 63.49; H, 5.88; N, 7.43.

Boc-(L-Phe-L-Oxd)$_2$-OH 5. Compound **4** (0.40 mmol, 0.30 g) was dissolved in MeOH (30 mL) under nitrogen. C/Pd (35 mg, 10% w/w) was added under nitrogen. A vacuum was created inside the flask using the vacuum line. The flask was then filled with hydrogen using a balloon (1 atm). The solution was stirred for 16 h in a hydrogen atmosphere. The product was obtained pure in 97% yield (0.26 g) as a waxy solid, after filtration through filter paper and concentration in vacuo. ^1H NMR (CD_3OD): δ 1.15−1.30 (m, 9H, *t*-Bu), 1.37−1.48 (m, 6H, 2 × Me), 2.48 (dd, 1H, *J* = 10.8, 14.0 Hz, C*H*H-Ph), 2.77 (dd, 1H, *J* = 10.4, 14.4 Hz, C*H*H-Ph), 3.10−3.33 (m, 2H, 2 × CH*H*-Ph), 4.44−4.52 (m, 2H, 2 × CHN-Oxd), 4.61−4.69 (m, 2H, 2 × CHO-Oxd), 5.32−5.39 (m, 1H, NH), 5.65−5.74 (m, 1H, NH), 7.05−7.33 (m, 10H, 2 × Ph). ^{13}C NMR (CD_3OD): δ 20.6, 28.6, 37.4, 38.0, 55.3, 56.1, 63.0, 63.3, 76.2, 76.4, 80.6, 127.6, 127.8, 129.2, 130.4, 137.8, 138.5, 163.8, 154.1, 158.0, 170.1, 171.4, 173.0, 174.1. Anal. Calcd for $C_{33}H_{38}N_4O_{11}$: C, 59.45; H, 5.75; N, 8.40. Found: C, 59.41; H, 5.74; N, 8.38.

Boc-(L-Phe-L-Oxd)$_3$-OBn 6. A solution of **5** (0.168 g, 0.25 mmol) and HBTU (0.095 g, 0.25 mmol) in dry acetonitrile (20 mL) was stirred in a nitrogen atmosphere for 10 min at room temperature. Then a mixture of **3** (0.25 mmol) and Et_3N (0.75 mmol, 0.104 mL) in dry acetonitrile (10 mL) was added dropwise at room temperature. The solution was stirred for 50 min in a nitrogen atmosphere, and then acetonitrile was removed under reduced pressure and replaced with ethyl acetate. The mixture was washed with brine (1 × 30 mL), 1 N aqueous HCl (1 × 30 mL), and a concentrated solution of $NaHCO_3$ (1 × 30 mL), dried over sodium sulfate, and concentrated in vacuo. For the purification from tetramethylurea and the byproduct, the residue was suspended in cyclohexane and sonicated for 15 min to dissolve the byproduct. Compound **6** was filtered, dried in vacuo, and obtained pure in 73% yield (0.18 g) as a white solid. Mp: 79−80 °C. $[\alpha]_D^{20}$: −30 (*c* 0.3, $CHCl_3$). IR (CH_2Cl_2, 3 mM): ν 3442, 1789, 1752, 1718 cm^{-1}. IR (solid, 1% in KBr): ν 3371, 1788, 1754, 1714 cm^{-1}. ^1H NMR ($CDCl_3$): δ 1.05−1.68 (m, 18H, 3 × Me + *t*-Bu), 2.58−2.94 (m, 3H, 3 × C*H*H-Ph), 3.27−3.51 (m, 3H, 3 × CH*H*-Ph), 4.20−4.87 (m, 6H, 3 × CHN-Oxd + 3 × CHO-Oxd), 4.94 (bs, 1H, NH), 5.05−5.18 (m, 2H, OCH_2Ph), 5.82−6.07 (m, 3H, 3 × C*H*N-CH_2Ph), 6.75 (bs, 1H, NH), 6.89−7.47 (m, 25H, 5 × Ph), 7.17 (bs, 2H, 2 × NH), 7.34 (bs, 1H, NH). ^{13}C NMR ($CDCl_3$): δ 20.3, 21.1, 27.8, 28.2, 37.2, 37.7, 53.1, 54.3, 60.3, 61.7, 62.7, 63.0, 68.2, 74.0, 74.2, 74.4, 80.0, 126.9, 127.1, 128.4, 128.8, 129.2, 129.6, 129.9, 134.5, 135.9, 151.0, 151.7, 155.2, 155.6, 167.0, 167.6, 171.1, 171.4. Anal. Calcd for $C_{54}H_{58}N_6O_{15}$: C, 62.90; H, 5.67; N, 8.15. Found: C, 62.87; H, 5.65; N, 8.18.

H-(L-Phe-L-Oxd)$_2$-OBn·CF_3CO_2H 7. A solution of **2** (0.52 mmol, 0.39 g) and TFA (9.36 mmol, 0.720 mL) in dry methylene chloride (20 mL) was stirred at room temperature for 4 h; then the volatiles were removed under reduced pressure, and the corresponding amine salt was obtained pure in 96% yield (0.38 g) as a waxy solid. ^1H NMR ($CDCl_3$): δ 1.34−1.52 (m, 6H, 2 × Me), 2.49−2.90 (m, 2H, 2 × C*H*H-Ph), 3.01−3.35 (m, 2H, 2 × CH*H*-Ph), 4.19−4.68 (m, 4H, 2 × CHN-Oxd + 2 × CHO-Oxd), 4.89−5.18 (m, 1H, NH), 5.30−5.81 (m, 2H, 2 × C*H*N-CH_2Ph), 7.05−7.35 (m, 15H, 3 × Ph). ^{13}C NMR ($CDCl_3$): δ 20.5, 20.9, 27.7, 28.1, 36.1, 36.6, 37.7, 38.8, 53.2, 53.7, 54.3, 55.5, 61.5, 62.2, 68.4, 74.4, 127.1, 127.3, 128.5, 128.7, 128.8, 129.0, 129.3, 129.5, 129.6, 134.3, 134.8, 151.7, 159.4 (q, CF_3), 167.5, 171.1. Anal. Calcd for $C_{37}H_{37}F_3N_4O_{11}$: C, 57.66; H, 4.84; N, 7.27. Found: C, 57.68; H, 4.83; N, 7.30.

Boc-(L-Phe-L-Oxd)$_4$-OBn 8. A solution of **5** (0.16 g, 0.24 mmol) and HBTU (0.091 g, 0.24 mmol) in dry acetonitrile (20 mL) was stirred in a nitrogen atmosphere for 10 min at room temperature. Then a mixture of **3** (0.24 mmol) and Et_3N (0.72 mmol, 0.100 mL) in dry acetonitrile (10 mL) was added dropwise at room temperature. The solution was stirred for 50 min in a nitrogen atmosphere, and then acetonitrile was removed under reduced pressure and replaced with ethyl acetate. The mixture was washed with brine (1 × 30 mL), 1 N aqueous HCl (1 × 30 mL), and a concentrated solution of $NaHCO_3$ (1 × 30 mL), dried over sodium sulfate, and concentrated in vacuo. For the purification from tetramethylurea and the byproduct, the residue was suspended in cyclohexane and sonicated for 15 min to dissolve the byproduct. Compound **8** was filtered, dried in vacuo, and obtained pure in 70% yield (0.22 g) as a white solid. Mp: 87−88 °C. $[\alpha]_D^{20}$: −28.0 (*c* 1.0, $CHCl_3$). IR (CH_2Cl_2, 3 mM): ν 3428, 1789, 1707 cm^{-1}. IR (solid, 1% in KBr): ν 3361, 1791, 1749, 1714 cm^{-1}. ^1H NMR ($CDCl_3$): δ 1.10−1.38 (m, 21H, 4 × Me + *t*-Bu), 2.71−3.30 (m, 8H, 4 × C*H*$_2$-Ph), 4.07−4.64 (m, 8H, 4 × CHN-Oxd + 4 × CHO-Oxd), 4.79−5.17 (m, 3H, OC*H*$_2$Ph + NH), 5.40−6.13 (m, 4H, 4 × C*H*N-CH_2Ph), 6.98−7.33 (m, 28H, 5 × Ph + 3 × NH), 7.47 (bs, 1H, NH). ^{13}C NMR ($CDCl_3$): δ 20.3, 20.6, 20.9, 28.3, 37.0, 37.8, 38.4, 53.1, 53.7, 54.1, 61.7, 62.7, 68.3, 73.9, 74.5, 74.9, 79.9, 126.8, 126.9, 127.2, 127.4, 128.4, 128.5, 128.8, 129.7, 134.5, 135.5, 136.0, 151.3, 151.8, 152.1, 155.2, 167.3, 168.0, 171.3. Anal. Calcd for $C_{68}H_{72}N_8O_{19}$: C, 62.57; H, 5.56; N, 8.58. Found: C, 62.55; H, 5.54; N, 8.61.

Boc-(L-Phe-L-Oxd)$_4$-OH 9. Compound **8** (0.30 mmol, 0.36 g) was dissolved in MeOH (30 mL) under nitrogen. C/Pd (35 mg, 10% w/w) was added under nitrogen. A vacuum was created inside the flask using the vacuum line. The flask was then filled with hydrogen using a balloon (1 atm). The solution was stirred for 16 h under a hydrogen atmosphere. The product was obtained pure in 98% yield (0.28 g) as a white solid, after filtration through filter paper and concentration in vacuo. Mp: 76 °C. ^1H NMR ($CDCl_3$): δ 1.20−1.61 (m, 21H, 4 × Me + *t*-Bu), 2.52−2.68 (m, 1H, 1 × C*H*H-Ph), 2.72−3.02 (m, 3H, 1 × C*H*H-Ph, 2 × CH*H*-Ph), 4.46−4.83 (m, 6H, 3 × CHN-Oxd + 3 × CHO-Oxd), 5.44−5.94 (m, 4H, 4 × C*H*N-CH_2Ph), 7.12−7.56 (m, 20H, 4 × Ph). ^{13}C NMR (CD_3OD): δ 19.2, 19.9, 35.8, 36.0, 36.6, 53.0, 54.8, 61.8, 62.0, 75.1, 76.3, 79.3, 126.4, 127.9, 128.0, 129.0, 136.6, 137.2, 152.2, 152.6, 169.1, 171.4, 171.6, 172.8. Anal. Calcd for $C_{61}H_{66}N_8O_{19}$: C, 60.29; H, 5.47; N, 9.22. Found: C, 60.32; H, 5.46; N, 9.20.

Boc-(L-Phe-L-Oxd)$_6$-OBn 10. A solution of **9** (0.13 g, 0.11 mmol) and HBTU (0.09 g, 0.11 mmol) in dry acetonitrile (20 mL) was stirred in a nitrogen atmosphere for 10 min at room temperature. Then a mixture of **7** (0.09 g, 0.11 mmol) and Et_3N (0.33 mmol, 0.05 mL) in dry acetonitrile (15 mL) was added dropwise at room temperature. The solution was stirred for 50 min in a nitrogen atmosphere, and then acetonitrile was removed under reduced pressure and replaced with ethyl acetate. The mixture was washed with brine (1 × 30 mL), 1 N aqueous HCl (1 × 30 mL), and a concentrated solution of $NaHCO_3$ (1 × 30 mL), dried over sodium sulfate, and concentrated in vacuo. For the purification from tetramethylurea and the byproduct, the residue was suspended in cyclohexane and sonicated for 15 min to dissolve the byproduct. Compound **9** was filtered, dried in vacuo, and obtained pure as a white solid in 68% (0.14 g) yield. Mp: 92−93 °C. $[\alpha]_D^{20}$: −30 (*c* 1.0, $CHCl_3$). IR (CH_2Cl_2, 3 mM): ν 3411, 3328, 1789, 1733, 1699 cm^{-1}. IR (solid, 1% in KBr): ν 3330, 1790, 1747, 1701, 1650 cm^{-1}. ^1H NMR ($CDCl_3$): δ 0.97−1.64 (m, 27H, 6 × Me + *t*-Bu), 2.69−3.42 (m, 12H, 8 × C*H*$_2$-Ph), 4.11−4.75 (m, 12H, 6 × CHN-Oxd + 6 × CHO-Oxd), 5.01−5.77 (m, 3H, OC*H*$_2$Ph + NH), 5.39−6.11 (m, 6H, 6 × C*H*N-CH_2Ph), 6.67 (bs, 1H, NH), 6.93−7.45 (m, 39H, 7 × Ph + 4 × NH). ^{13}C NMR ($CDCl_3$): δ 13.1, 19.3, 19.7, 20.0, 27.7, 28.6, 35.7, 36.7, 37.3, 37.7, 51.9, 52.3, 52.6, 53.0, 60.7, 61.5, 61.6, 67.2, 72.8, 73.2, 74.0, 78.9, 125.8, 126.3, 127.5, 127.6, 127.7, 128.4, 128.6, 133.6, 134.4, 134.5, 134.8, 150.2, 150.9, 165.8, 166.3, 166.8, 170.2, 170.4, 170.6. Anal.

Calcd for $C_{96}H_{100}N_{12}O_{27}$: C, 62.20; H, 5.44; N, 9.07. Found: C, 62.22; H, 5.46; N, 9.11.

ECD Spectra. The CD spectra were recorded at room temperature on a spectropolarimeter. Quartz cuvettes of 0.01, 0.1, 1, and 2 cm path length were employed. Foldamers were dissolved in methanol yielding clear approximately 1 mM solutions. The spectra were scanned between 190 and 300 nm for the far-UV and near-UV regions, with 0.2 nm resolution. Thirty-six scans were collected with a scanning speed of 50 nm min^{-1} and a time constant of 1 s, and the solvent baseline was subtracted from the averaged spectra. Final spectra are presented in molar ellipticity. Spectral analysis was performed by fitting the measured spectra in the far-UV spectra with reference spectra based on the CD curves of different model peptides with varying amounts of α-helix, β-sheet, β-turn, and random coil conformations. Reference spectra were described by J. Reed and T. A. Reed for peptide analysis.[32]

IR and VCD Spectra. IR and VCD spectra of Figure 5 and 7 were measured at a resolution of 4 cm^{-1} in the mid-IR region from about 900 to 1850 cm^{-1}. Foldamers (monomers to hexamers) were dissolved in methanol-d_4 and in CCl_4 (monomers) at a concentration of 0.02 M in an IR liquid cell with a path length of 0.2 mm. All the VCD spectra reported were measured with a collection time of 1 h. In all cases, the spectrum of the solvent was subtracted from the IR and VCD spectra. For $n = 1$ in CCl_4, both enantiomers have been measured to check the VCD data reliability.

Computational Methods. Conformational searches have been conducted, first at the PM3 level, and then at the B3LYP/6-31+G** level, with GAUSSIAN09.[33] Harmonic frequencies, dipole strengths, and rotational strengths have been calculated, following normal-mode analysis and the magnetic-field perturbation method to calculate rotational strengths for conformational energy minima. From these data, IR and VCD spectra were generated by assigning a Lorentzian band shape to each fundamental vibrational transition with a half-width of 12 cm^{-1}. Centerband frequencies were shifted by multiplying by a 0.98 constant factor to facilitate comparison with experimental spectra.

■ ASSOCIATED CONTENT

Supporting Information

Variation of the NH proton chemical shifts (ppm) of **6**, **8**, and **10**; X-ray powder diffraction (XRD) patterns for **4**, **6**, **8**, and **10**; ECD spectra of **1**, **4**, **6**, **8**, and **10** in MeOH solution; IR and VCD spectra of **1**, **4**, **6**, **8**, and **10** in CD_3OD; characteristics of the conformers obtained for compound **1**; calculated IR and VCD spectra of **1**, for the most populated conformers; calculated ECD spectra of **1** for the most populated conformers; Cartesian coordinates of optimized structures of **1** at the B3LYP/6-31+g(d,p) level for the four most populated conformers; copies of the ^1H and ^{13}C NMR spectra of oligomers **1**−**10**. This material is available free of charge via the Internet at http://pubs.acs.org.

■ AUTHOR INFORMATION

Corresponding Author

*Email: longhi@med.unibs.it, piera.sabatino@unibo.it, claudia.tomasini@unibo.it.

Notes

The authors declare no competing financial interest.

■ ACKNOWLEDGMENTS

We would like to thank "Ministero dell'Istruzione, dell'Università e della Ricerca" (MIUR) for financial support, under the auspices of the programs PRIN 2008LYSESR and PRIN 2008J4YNJY. We also thank CILEA (Consorzio Interuniversitario Lombardo Elaborazione Automatica) for access to their computational facilities and Fondazione del Monte di Bologna e di Ravenna for financial support.

■ REFERENCES

(1) (a) Hill, D. J.; Mio, M. J.; Prince, R. B.; Hughes, T. S.; Moore, J. S. *Chem. Rev.* **2001**, *101*, 3893−4011. (b) *Foldamers: Structure, Properties, and Applications*; Hecht, S., Huc, I., Eds.; Wiley-VCH: Weinheim, Germany, 2007.

(2) Gellman, S. H. *Acc. Chem. Res.* **1998**, *31*, 173−180.

(3) (a) Martinek, T. A.; Fülöp, F. *Chem. Soc. Rev.* **2012**, *41*, 687−702. (b) Cubberley, M. S.; Iverson, B. L. *Curr. Opin. Chem. Biol.* **2001**, *5*, 650−653. (c) Seebach, D.; Beck, A. K.; Bierbaum, D. J. *Chem. Biodiversity* **2004**, *1*, 1111−1239. (d) Sanford, A.; Yamato, K.; Yang, X. W.; Yuan, L. H.; Han, Y. H.; Gong, B. *Eur. J. Biochem.* **2004**, *271*, 1416−1425. (e) Cheng, R. P. *Curr. Opin. Struct. Biol.* **2004**, *14*, 512−520. (f) Balbo Block, M. A.; Kaiser, C.; Khan, A.; Hecht, S. *Top. Curr. Chem.* **2005**, *245*, 89−150. (g) Goodman, C. M.; Choi, S.; Shandler, S.; DeGrado, W. F. *Nat. Chem. Biol.* **2007**, *3*, 252−262. (h) Bautista, A. D.; Craig, C. J.; Harker, E. A.; Schepartz, A. *Curr. Opin. Chem. Biol.* **2007**, *11*, 685−692. (i) Smaldone, R. A.; Moore, J. S. *Chem.−Eur. J.* **2008**, *14*, 2650−2657. (j) Guichard, G.; Huc, I. *Chem. Commun.* **2011**, *47*, 5933−5941.

(4) Tomasini, C.; Angelici, G.; Castellucci, N. *Eur. J. Org. Chem.* **2011**, 3648−3669.

(5) (a) Tomasini, C.; Villa, M. *Tetrahedron Lett.* **2001**, *42*, 5211−5214. (b) Bernardi, F.; Garavelli, M.; Scatizzi, M.; Tomasini, C.; Trigari, V.; Crisma, M.; Formaggio, F.; Peggion, C.; Toniolo, C. *Chem.−Eur. J.* **2002**, *8*, 2516−2525.

(6) (a) Luppi, G.; Soffrè, C.; Tomasini, C. *Tetrahedron: Asymmetry* **2004**, *15*, 1645−1650. (b) Tomasini, C.; Luppi, G.; Monari, M. *J. Am. Chem. Soc.* **2006**, *128*, 2410−2420. (c) Angelici, G.; Luppi, G.; Kaptein, B.; Broxterman, Q. B.; Hofmann, H.-J.; Tomasini, C. *Eur. J. Org. Chem.* **2007**, 2713−2721.

(7) (a) Angelici, G.; Falini, G.; Hofmann, H.-J.; Huster, D.; Monari, M.; Tomasini, C. *Angew. Chem., Int. Ed.* **2008**, *47*, 8075−8078. (b) Angelici, G.; Falini, G.; Hofmann, H.-J.; Huster, D.; Monari, M.; Tomasini, C. *Chem.−Eur. J.* **2009**, *15*, 8037−8048.

(8) (a) Detoma, A. S.; Salamekh, S.; Ramamoorthy, A.; Lim, M. H. *Chem. Soc. Rev.* **2012**, *41*, 608−621. (b) Ryan, D. M.; Nilsson, B. L. *Polym. Chem.* **2012**, *3*, 18−33. (c) Woolfson, D. N. *Biopolymers* **2010**, *94*, 118−127. (d) Woolfson, D. N.; Ryadnov, M. G. *Curr. Opin. Chem. Biol.* **2006**, *10*, 559−567. (e) Serpell, L. C. *Biochim. Biophys. Acta* **2000**, *1502*, 16−30.

(9) (a) Ross, C. A.; Poirier, M. A. *Nat. Med. (Tokyo, Jpn.)* **2004**, *10*, S10−S17. (b) Dalakas, M. C. *Neuropathol. Appl. Neurobiol.* **2011**, *37*, 226−242. (c) Filosto, M.; Scarpelli, M.; Cotelli, M. S.; Vielmi, V.; Todeschini, A.; Gregorelli, V.; Tonin, P.; Tomelleri, G.; Padovani, A. *J. Neurol.* **2011**, *258*, 1763−1774. (d) Bekris, L. M.; Bird, C.-E. T. D.; Tsuang, D. W. *Journal of Geriatric Psychiatry Neurology* **2010**, *23*, 213−227.

(10) (a) Colletier, J.-P.; Laganowsky, A.; Landau Meytal, M.; Zhao, M. L.; Soriaga, A. B.; Goldschmidt, L.; Flot, D.; Cascio, D.; Sawaya, M. R.; Eisenberg, D. *Proc. Natl. Acad. Sci. U.S.A.* **2011**, *108*, 16938−16943. (b) Makin, O. S.; Serpell, L. C. *FEBS J.* **2005**, *272*, 5950−5961. (c) McLaurin, J.; Yang, D. S.; Yip, C. M.; Fraser, P. E. *J. Struct. Biol.* **2000**, *130*, 259−270.

(11) Tomasini, C.; Trigari, V.; Lucarini, S.; Bernardi, F.; Garavelli, M.; Peggion, C.; Formaggio, F.; Toniolo, C. *Eur. J. Org. Chem.* **2003**, 259−267.

(12) (a) Belvisi, L.; Gennari, C.; Mielgo, A.; Potenza, D.; Scolastico, C. *Eur. J. Org. Chem.* **1999**, 389−400. (b) Yang, J.; Gellman, S. H. *J. Am. Chem. Soc.* **1998**, *120*, 9090−9091. (c) Jones, I. G.; Jones, W.; North, M. *J. Org. Chem.* **1998**, *63*, 1505−1513. (d) Toniolo, C.; Benedetti, E. *Crit. Rev. Biochem.* **1980**, *9*, 1−44. (e) Imperiali, B.; Moats, R. A.; Fisher, S. L.; Prins, T. J. *J. Am. Chem. Soc.* **1992**, *114*, 3182−3188.

(13) (a) Kopple, K. D.; Ohnishi, M.; Go, A. *Biochemistry* **1969**, *8*, 4087−4095. (b) Martin, D.; Hauthal, G. G. In *Dimethyl Sulphoxide*; Van Nostrand-Reinhold: Wokingham, U.K., 1975.

(14) Stevens, E. S.; Sugawara, N.; Bonora, G. M.; Toniolo, C. *J. Am. Chem. Soc.* **1980**, *102*, 7048−7050.
(15) Sreerama, N.; Manning, M. C.; Powers, M. E.; Zhang, J.-X.; Goldenberg, D. P.; Woody, R. W. *Biochemistry* **1999**, *38*, 10814−10822.
(16) Tatham, A. S.; Drake, A. F.; Shewry, P. R. *Biochem. J.* **1989**, *259*, 471−476 and references therein.
(17) Krysmann, M. J.; Castelletto, V.; McKendrick, J. E.; Clifton, L. A.; Hamley, I. W.; Harris, P. J. F.; King, S. M. *Langmuir* **2008**, *24*, 8158−8162.
(18) (a) Holzwarth, G.; Hsu, E. C.; Mosher, H. S.; Faulkner, T. R.; Moscowitz, A. *J. Am. Chem. Soc.* **1974**, *96*, 251−252. (b) Sugeta, H.; Marcott, C.; Faulkner, T. R.; Overend, J.; Moscowitz, A. *Chem. Phys. Lett.* **1976**, *40*, 397−398.
(19) (a) Nafie, L. A.; Cheng, J. C.; Stephens, P. J. *J. Am. Chem. Soc.* **1975**, *97*, 3842−3843. (b) Nafie, L. A.; Keiderling, T. A.; Stephens, P. J. *J. Am. Chem. Soc.* **1976**, *98*, 2715−2723.
(20) Nafie, L. A. *Vibrational Optical Activity: Principles and Applications*; Wiley: New York, 2011.
(21) Stephens, P. J.; Devlin, F. J. *Chirality* **2000**, *12*, 172−179.
(22) Keiderling, T. A. Peptide and Protein Conformational Studies with Vibrational Circular Dichroism and Related Spectroscopies. In *Circular Dichroism Principles and Applications*, 2nd ed.; Berova, N., Nakanishi, K., Woody, R., Eds.; Wiley-VCH: New York, 2000; pp 621−666.
(23) Polavarapu, P. L. *Vibrational Spectra and Structure*; Bist, H. D., Durig, J. R., Sullivan, J. F., Eds.; Elsevier: Amsterdam, 1989; Vol. *17B*, pp 319−342.
(24) Uncuta, C.; Bartha, E.; Gherase, D.; Teodorescu, F.; Draghici, C.; Cavagnat, D.; Daugey, N.; Liotard, D.; Buffeteau, T. *Chirality* **2010**, *22*, E115−E122.
(25) (a) Longhi, G.; Abbate, S.; Gangemi, R.; Giorgio, E.; Rosini, C. *J. Phys. Chem. A* **2006**, *110*, 4958−4968. (b) Abbate, S.; Castiglioni, E.; Gangemi, F.; Gangemi, R.; Longhi, G.; Ruzziconi, R.; Spizzichino, S. *J. Phys. Chem. A* **2007**, *111*, 7031−7040.
(26) Cantor, C. R.; Schimmel, P. R. *Biophysical Chemistry*; W. H. Freeman and Co.: San Francisco, 1980.
(27) Baumruk, V.; Huo, D.; Dukor, R. K.; Keiderling, T. A.; Lelievre, D.; Brack, A. *Biopolymers* **1994**, *34*, 1115−1121.
(28) Keiderling, T. A. Vibrational Circular Dichroism of Proteins. In *Spectroscopic Methods for Protein Structure Determination*; Havel, H. A., Ed.; Wiley-VCH: New York, 1998.
(29) Eker, F.; Gribenow, K.; Cao, X.; Schweitzer-Stenner, R. *Proc. Natl. Acad. Sci. U.S.A.* **2004**, *101*, 10054−10059.
(30) Paterlini, M. G.; Freedman, T. B.; Nafie, L. A. *Biopolymers* **1986**, *25*, 1751−1765.
(31) (a) Yasui, S. C.; Keiderling, T. A. *J. Am. Chem. Soc.* **1986**, *108*, 5576−5581. (b) Dukor, R. K.; Keiderling, T. A. *Biopolymers* **1991**, *31*, 1747−1761.
(32) Reed, J.; Reed, T. A. *Anal. Biochem.* **1997**, *254*, 36−40.
(33) Frisch, M. J.; Trucks, G. W.; Schlegel, H. B.; Scuseria, G. E.; Robb, M. A.; Cheeseman, J. R.; Scalmani, G.; Barone, V.; Mennucci, B.; Petersson, G. A.; Nakatsuji, H.; Caricato, M.; Li, X.; Hratchian, H. P.; Izmaylov, A. F.; Bloino, J.; Zheng, G.; Sonnenberg, J. L.; Hada, M.; Ehara, M.; Toyota, K.; Fukuda, R.; Hasegawa, J.; Ishida, M.; Nakajima, T.; Honda, Y.; Kitao, O.; Nakai, H.; Vreven, T.; Montgomery, J. A., Jr.; Peralta, J. E.; Ogliaro, F.; Bearpark, M.; Heyd, J. J.; Brothers, E.; Kudin, K. N.; Staroverov, V. N.; Kobayashi, R.; Normand, J.; Raghavachari, K.; Rendell, A.; Burant, J. C.; Iyengar, S. S.; Tomasi, J.; Cossi, M.; Rega, N.; Millam, J. M.; Klene, M.; Knox, J. E.; Cross, J. B.; Bakken, V.; Adamo, C.; Jaramillo, J.; Gomperts, R.; Stratmann, R. E.; Yazyev, O.; Austin, A. J.; Cammi, R.; Pomelli, C.; Ochterski, J. W.; Martin, R. L.; Morokuma, K.; Zakrzewski, V. G.; Voth, G. A.; Salvador, P.; Dannenberg, J. J.; Dapprich, S.; Daniels, A. D.; Farkas, Ö.; Foresman, J. B.; Ortiz, J. V.; Cioslowski, J.; Fox, D. J. *Gaussian 09*; revision A.1; Gaussian, Inc.: Wallingford, CT, 2009.